Low-Generation Cationic Phosphorus Dendrimers: Novel Approach to Tackle Drug-Resistant S. aureus In Vitro and In Vivo

Evgeny Apartsin, Abdul Akhir, Grace Kaul, Deepanshi Saxena, Regis Laurent, Kishore Kumar Srivastava, Serge Mignani, Jean-Pierre Majoral, Sidharth Chopra

Title: Low-generation cationic phosphorus dendrimers: Novel approach to tackle drug-resistant *S. aureus in vitro* and *in vivo*

Authors: Evgeny Apartsin [1,2]*, Abdul Akhir[3], Grace Kaul[3,4] Deepanshi Saxen[3], Regis Laurent[1], Kishore Kumar Srivastava[3], Serge Mignani[5,6]*, , Jean-Pierre Majoral[1,*] and Sidharth Chopra[3,4]*

Affiliation: [1]Laboratoire de Chimie de Coordination du CNRS, 205 Route de Narbonne, BP 44099, 31077 Toulouse Cedex 4, France; and LCC-CNRS, Université de Toulouse, CNRS, 31400 Toulouse, France;

[2] Univ.Bordeaux,CNRS,Bordeaux INP,CBMM,UMR5248F-33600 Pessac,France

[3]Division of Molecular Microbiology and Immunology, CSIR-Central Drug Research Institute, Sitapur Road, Sector 10, Janakipuram Extension, Lucknow-226031, Uttar Pradesh, India;

[4]Academy of Scientific and Innovative Research (AcSIR), Ghaziabad-201002, India;

[5]UNICAEN, CERMN (Centre d'Etudes et de Recherche sur le Medicament de Normandie), 14032 Caen, France

[6]CQM—Centro de Quimica da Madeira, MMRG, Campus da Penteada, Universidade da Madeira, 9020-105 19, Funchal, Portugal.

* These authors contributed equally to the manuscript.

@To whom correspondence should be addressed

Dr. Sidharth Chopra, Principal Scientist, Division of Molecular Microbiology and Immunology, CSIR-Central Drug Research Institute, Sitapur Road, Sector 10, Janakipuram Extension, Lucknow-226031, Uttar Pradesh, India. Email: Skchopra007@gmail.com, ORCID: 0000-0001-8823-6074

Evgeny Apartsin: Laboratoire de Chimie de Coordination du CNRS, 205 Route de Narbonne, BP 44099, 31077 Toulouse Cedex 4, France; LCC-CNRS, Université de Toulouse, CNRS, 31400 Toulouse, France; ORCID : 0000-0003-3334-0397, Email : eapartsin@gmail.com

Dr. Jean-Pierre Majoral: Laboratoire de Chimie de Coordination du CNRS, 205 Route de Narbonne, BP 44099, 31077 Toulouse Cedex 4, France; LCC-CNRS, Université de Toulouse, CNRS, 31400 Toulouse, France; Email: jean-pierre.majoral@lcc-toulouse.fr Orcid: 0000-0002-0971-817X

Dr. Serge Mignani: UNICAEN, CERMN (Centre d'Etudes et de Recherche sur le Medicament de Normandie), 14032 Caen, France; CQM—Centro de Quimica da Madeira, MMRG, Campus da Penteada, Universidade da Madeira, 9020-105 19, Funchal, Portugal; Email: serge.mignani@paris, serge.mignani@staff.uma.pt, ORCID: 0000-0002-1383-5256

Keywords: Polycationic-phosphorous dendrimers, AMR, MRSA, fluorescence microscopy, resistance, SEM.

Abstract

The incessant, global increase in antimicrobial resistance (AMR) is a very big challenge for healthcare systems. AMR is predicted to grow at an alarming pace, with a dramatic increase in morbidity, mortality and US$ 100 trillion loss to the global economy by 2050. The mortality rate caused due to methicillin-resistant *S. aureus* (MRSA) is much higher as compared to infections caused due to drug-susceptible *S. aureus*. Additionally, there is a big paucity of therpeutics available for treatment of serious infections caused due to MRSA Thus, urgent discovery and development of novel therapies is an urgent, unmet medical need. In this context, we synthesized AE4G0, a low-generation cationic-phosphorus dendrimer expressing potent antimicrobial activity against *S. aureus* and *Enterococcus* sp., and demonstrating a broad selectivity index against eukaryotic cells. AE4G0 exhibits concentration-dependent, bactericidal activity and synergizes with gentamicin, especially against gentamicin-resistant MRSA NRS119. Fluorescence and scanning electron microscopy demonstrate that treatment with AE4G0 led to the utter destruction of *S. aureus* ATCC 29213 without inducing resistance, despite repeated exposure. When tested *in vivo*, AE4G0 demonstrates significant efficacy against *S. aureus* ATCC 29213, alone and in combination with gentamicin against gentamicin-resistant *S. aureus* NRS119 in the murine skin model of infection. Taken together, AE4G0 demonstrates the potential to be translated as a novel therapeutic option for the treatment of topical, drug-resistant *S. aureus* infections.

Introduction

AMR is emerging and spreading at an alarming pace, thus adversely affecting healthcare systems globally. Uncontrolled and inappropriate antibiotic use are some of the leading causes of the expansion of multidrug-resistant (MDR) strains predicted to be responsible for ~700,000 annual deaths and a US$ 100 trillion loss to the global economy by 2050[1]. Among the top World Health Organisation (WHO) priority pathogens for which novel therapeutic options are urgently required, *Staphylococcus aureus*, a gram-positive bacteria that mainly inhabits human skin and mucous membranes, is one of the main causative agents for community and hospital-acquired infections including endocarditis, skin and soft tissue infections, bacteraemia, osteomyelitis and life-threatening pneumonia[2]. In fact, infection with MRSA leads to

64% more chance of death as compared to infection with drug-susceptible *S. aureus[3]*. Since MRSA and vancomycin-resistant *S. aureus* (VRSA) are WHO high priority pathogens, thus, discovery and development of new antibiotics is an urgent, unmet medical need[4].

In this context, highly branched tree-like polymers, called dendrimers, are characterized by precisely defined structures and molecular weights. Due to their multivalency, polyvalent interactions with cellular and molecular targets have been observed[5-7]. Many publications report neutral, anionic or cationic phosphorus dendrimers as exhibiting anti-tumoral[8-10], anti-tubercular[11], anti-inflammatory[12-16],effect on prion or Alzheimer's diseases[17] or for the formation of a variety of hydrogels[18]. Surprisingly, anti-bacterial activities of these phosphorus dendrimers have not been investigated in detail. In an exception, a recent report describes synergistic effects of a polyanionic phosphorus dendrimer of generation 4 bearing 96-end carboxylic groups to synergize with levofloxacin, potentially leading to reduced antibiotic dose for treatment of bacterial infection[19]. Therefore, it was of great interest to explore the antimicrobial properties of original, polycationic phosphorus dendrimers of low generation and more intensively, of AE4G0. AE4G0 was tested against highly drug-resistant MRSA, VRSA along with *Enterococcus spp*. Various pre-clinical parameters of AE4G0 were determined, followed by *in vivo* potential in a murine model of skin infection alone and in combination with gentamicin against *S. aureus* ATCC 29213 and gentamicin-resistant MRSA NRS119.

Materials and Methods

Materials

All manipulations were carried out using a standard dry argon-high vacuum technique. Organic solvents were dried and freshly distilled under argon prior to use. Reagents were obtained from commercial sources and used as received. Compound **(1)** was synthesized from chloroacetic acid by standard esterification upon acid catalysis. Compounds **(3a,b)** (so-called Girard reagents P and T) were obtained from commercial sources and used as received.

Analytical and spectroscopic techniques

^{1}H, $^{13}C\{^{1}H\}$ and $^{31}P\{^{1}H\}$ NMR spectra were recorded on Bruker AV400PAS and AV300PAS (Bruker, Karlsruhe, Germany) instruments. ^{1}H and ^{13}C chemical shifts (δ, ppm) were measured relative to residual resonances of solvents. High-resolution mass spectra were recorded using GCT Premier (Waters, Milford, MA, USA) and UPLC Xevo G2 Q TOF (Waters, Milford, MA, USA) mass spectrometers for chemical ionization and electrospray ionization, respectively.

Dendrimers synthesis

Aldehyde-terminated dendrimer (**4**) (0.46 mmol) was dissolved in 20 mL $CHCl_3$, then solution of an acetohydrazide (2.83 mmol) in 20 mL methanol was added. Reaction mixture was acidified to pH~5 with acetic acid and stirred overnight at 45 ˚C. Once 1H NMR confirmed the completeness of aldehyde conversion into hydrazone, the solvent was removed, and the solid residue was washed with $CHCl_3$ and diethyl ether, then dried.

Pyridinium-terminated dendrimer PG0

Pale powder, yield: 95%. ^{1}H NMR (400 MHz, DMSO-d6) δ, ppm: 5.76, 6.18 (2d, J = 13.8 Hz, 12H, C(O)-CH_2-N), 7.08 (m, 12H, CH-C-CH=N), 7.63 (m, 12H, O-C-CH), 8.21 (q, J = 7.1 Hz, 12H, pyridinium), 8.30 – 8.54 (m, 6H, CH=N), 8.68 (q, J = 7.7 Hz, 6H, pyridinium), 9.23 (m, 12H, pyridinium), 12.49, 12.63, 13.29 (3br s, 6H, N-NH). $^{13}\{^{1}H\}$C NMR (101 MHz, DMSO) □, ppm: 61.36, 61.74 (d, J = 11.4 Hz), 121.40, 127.94 (dd, J = 17.8, 7.7 Hz), 129.12 (d, J = 18.2 Hz), 131.70, 144.71 (d, J = 11.6 Hz), 146.50 – 146.89 (m), 147.06, 147.50 (d, J = 16.1 Hz), 151.21, 161.88 (d, J = 11.7 Hz), 166.77 (d, J = 18.9 Hz), 172.44. $^{31}P\{^{1}H\}$ NMR (162 MHz, DMSO-d6) δ, ppm: 8.5 (m).

Trimethylammonium-terminated dendrimer AE4G0

Pale powder, yield: 95%. ^{1}H NMR (400 MHz, DMSO-d6) δ, ppm: 3.30 – 3.46 (m, 54H, N-CH_3), 4.48, 4.90 (2d, J = 11.9 Hz, 12H, C(O)-CH_2-N), 6.94 – 7.21 (m, 12H, CH-C-CH=N), 7.50 – 7.74 (m, 12H, O-C-CH), 8.28 – 8.50 (m, 6H, CH=N), 12.11 – 13.40 (m, 6H, N-NH). $^{13}\{^{1}H\}$C NMR (101 MHz, DMSO) □, ppm: 53.3 – 54.4 (m), 62.5, 63.8, 65.4, 79.8, 120.7 – 122.0 (m), 128.9 – 129.7 (m), 131.1 – 132.1 (m), 144.9 (d, J = 15.0 Hz), 148.2 (d, J = 15.8 Hz), 151.4 (d, J = 25.6 Hz), 160.4, 165.2 – 166.0 (m), 172.4. $^{31}P\{^{1}H\}$ NMR (162 MHz, DMSO-d6) δ, ppm: 8.4 (m). ESI-TOF HRMS: $[M]^{2+}$ 770.8468 (calcd 770.8458), $[M]^{3+}$ 514.2347 (calcd 514.2332), $[M]^{4+}$ 385.9276 (calcd 385.9268), $[M]^{5+}$ 308.9439 (calcd 308.9430), $[M]^{6+}$ 257.9548 (calcd 257.9548).

Triethylammonium-terminated dendrimer NEt_3G0

Pale powder, yield: 90%. ^{1}H NMR (400 MHz, DMSO-d6) δ, ppm: 1.28 (dt, J = 19.1, 7.2 Hz, 54H, -CH3), 3.52, 3.62 (2d, J = 7.1 Hz, 36H), 4.31, 4.61 (2s, 12H, C(O)-CH_2-N), 7.06 (p, J = 10.9, 9.6 Hz, 12H, CH-C-CH=N), 7.48 – 7.78 (m, 12H, O-C-CH), 8.18 – 8.47 (m, 6H, CH=N), 12.32 - 13.63 (m, 6H, N-NH). $^{13}\{^{1}H\}$C NMR (101 MHz, DMSO) □, ppm: 8.05, 53.92, 54.43, 54.76, 55.93, 121.28 (d, J = 13.8 Hz), 129.37 (d, J = 10.9 Hz), 131.52, 144.95, 148.15, 151.49, 160.17, 165.46. $^{31}P\{^{1}H\}$

NMR (162 MHz, DMSO-d6) δ, ppm: 8.1 (m). ESI-TOF HRMS: $[M]^{2+}$ 897.9897 (calcd 897.9896), $[M]^{3+}$ 598.6618 (calcd 598.6614), $[M]^{4+}$ 449.2483 (calcd 449.2480), $[M]^{5+}$ 359.5996 (calcd 359.5999), $[M]^{6+}$ 299.8333 (calcd 299.8346).

1-methyl-piperidinium-terminated dendrimer C6MeG0

Pale powder, yield: 90%. ^{1}H NMR (400 MHz, DMSO-d6) δ, ppm: 1.53 (m, 12H, N-CH_2-CH_2-$\underline{CH_2}$-), 1.90 (m, 24H, N-CH_2-$\underline{CH_2}$-), 3.36 (s, 18H, CH_3-N), 3.43 – 3.87 (dm, 24H, 4H, N-$\underline{CH_2}$-CH_2-), 4.58, 4.87 (2m, 12H, C(O)-$\underline{CH_2}$-N), 7.03 (m, 12H, $\underline{CH}$-C-CH=N), 7.62 (m, 12H, O-C-$\underline{CH}$), 8.20 – 8.56 (m, 6H, CH=N), 12.16 – 12.60, 13.08 – 13.46 (2m, 6H, N-NH). ^{13}C{^{1}H} NMR (101 MHz, DMSO) □, ppm: 19.38 – 20.09 (m), 20.67 – 21.32 (m), 50.46, 61.38 – 62.31 (m), 121.22 (d, J = 38.8 Hz), 129.28 (d, J = 15.1 Hz), 131.45 (d, J = 12.7 Hz), 144.83, 148.29 (d, J = 19.0 Hz), 151.44 (d, J = 15.5 Hz), 160.22, 162.47, 165.43 (t, J = 9.4 Hz), 166.75, 168.47, 172.42.^{31}P{^{1}H} NMR (162 MHz, DMSO-d6) δ, ppm: 8.2 (m). ESI-TOF HRMS: $[M]^{2+}$891.4425 (calcd 891.4412), $[M]^{3+}$ 594.9662 (calcd 594.9644), $[M]^{4+}$ 446.2261 (calcd 446.2245), $[M]^{5+}$ 357.1830 (calcd 357.1812), $[M]^{6+}$ 297.8186 (calcd 297.8189).

Piperidinyl-terminated dendrimer C6HG0

Pale powder, yield: 80%. ^{1}H NMR (400 MHz, DMSO-d6) δ, ppm: 1.41 (m, 12H, N-CH_2-CH_2-$\underline{CH_2}$-), 1.55 (q, J = 5.7 Hz, 24H, N-CH_2-$\underline{CH_2}$-), 2.43 (d, J = 5.9 Hz, 24H, N-$\underline{CH_2}$-CH_2-), 3.06, 3.48 (2m, 12H, C(O)-CH_2-N), 7.00 (m, 12H, $\underline{CH}$-C-CH=N), 7.55 (m, 12H, O-C-$\underline{CH}$), 7.93, 8.33 (2m, 6H, CH=N), 11.12 (m, 6H, N-NH). ^{13}C{^{1}H} NMR (101 MHz, DMSO-d6) δ, ppm: 21.6, 24.0 and 24.2 (2s), 25.8 and 26.1 (2s), 54.4 and 54.7 (2s), 58.4, 61.9, 121.3 and 128.6 (2d), 132.2 (m), 141.9 (m), 146.6 (t, J = 11.9 Hz), 151.0 (d, J = 18.8 Hz), 166.7 and 171.4 (2s). ^{31}P{^{1}H} NMR (162 MHz, DMSO-d6) δ, ppm: 8.4 (m). ESI-TOF HRMS: $[M+2H]^{2+}$ 806.8448 (calcd 806.8458), $[M+3H]^{3+}$ 538.2329 (calcd 538.2332), $[M+4H]^{4+}$ 403.9258 (calcd 403.9268), $[M+5H]^{5+}$ 323.3423 (calcd 323.3430), $[M+6H]^{6+}$ 269.6193 (calcd 269.6205).

Pyrrolidinyl-terminated dendrimer C5HG0

Pale powder, yield: 85%. ^{1}H NMR (400 MHz, DMSO-d6) δ, ppm: 1.70 (dt, J = 24.1, 5.4, 24H, N-CH_2-$\underline{CH_2}$-), 2.58 (m, 24H, N-$\underline{CH_2}$-CH_2-), 3.21, 3.61 (2s, 12H, C(O)-CH_2-N), 7.02 (m, 12H, $\underline{CH}$-C-CH=N), 7.55 (m, 12H, O-C-$\underline{CH}$), 7.87 – 8.36 (m, 6H, CH=N), 11.17 (m, 6H, N-NH). ^{13}C{^{1}H} NMR (101 MHz, DMSO-d6) δ, ppm: 23.86 (d, J = 9.8 Hz), 54.11 (d, J = 30.9 Hz), 55.30, 58.67 (d, J = 4.6 Hz), 121.30, 128.78 (d, J = 41.1 Hz), 132.17, 141.94, 146.60 (d, J = 11.0 Hz), 151.10, 166.87, 171.69. ^{31}P{^{1}H} NMR (162 MHz, DMSO-d6) δ, ppm: 8.5 (m). ESI-TOF HRMS: $[M+2H]^{2+}$ 848.8912 (calcd 848.8850),

$[M+3H]^{3+}$ 566.5989 (calcd 566.5988), $[M+4H]^{4+}$ 425.2006 (calcd 425.2010), $[M+5H]^{5+}$ 340.3614 (calcd 340.3624), $[M+6H]^{6+}$ 283.6346 (calcd 283.8033).

Biphenyl-blocked aldehyde-terminated dendrimer (6)

Hexachlorocyclotriphosphazene (4 mmol) and K_2CO_3 (12 mmol) were mixed in 20 mL of distilled CH_3CN and cooled down with an ice bath. Solution of 2,2′-dihydroxybiphenyl (4 mmol) in 10 mL distilled CH_3CN was added dropwise, and reaction mixture was stirred overnight at 0˚C to yield *P,P*-dihydroxybiphenyl-*P′,P′,P″,P″*-tetrachlorocyclotriphosphazene (**5**) that was used at the next stage without further purification. $^{31}P\{^1H\}$ NMR (162 MHz, $CDCl_3$) δ, ppm: 12.8 (dd), 25.3 (d). 4-hydroxybenzaldehyde (16.8 mmol) and K_2CO_3 (20 mmol) were added, and the reaction mixture was stirred overnight at r.t. Once $^{31}P\{^1H\}$ NMR showed complete conversion of (**5)** into biphenyl-blocked aldehyde-terminated dendrimer (**6**), the solvent was removed. The solid residue was dissolved in CH_2Cl_2, and washed 3 times with 1M KOH and 3 times with brine. The organic layer was dried over Na_2SO_4 and concentrated into a solid residue that was washed with diethyl ether to give (**6**) as white crystals that were recovered on a filter and dried. Yield: 80%.

^1H NMR (400 MHz, DMSO-d6) δ, ppm: 6.89 (dt, J = 7.7, 1.7 Hz, 2H, biphenyl), 7.36 (d, J = 8.6 Hz, 8H, -CH-C-CHO), 7.41 – 7.52 (m, 4H, biphenyl), 7.67 (dd, J = 7.3, 2.1 Hz, 2H, biphenyl), 7.95 (d, J = 8.6 Hz, 8H, P-O-C-CH), 9.99 (s, 4H, -CHO). $^{13}C\{^1H\}$ NMR (101 MHz, DMSO-d6) δ, ppm: 121.8 (t, J = 2.6 Hz), 127.3, 128.1 (d, J = 1.6 Hz), 130.5, 130.8, 132.1, 134.2, 147.3, 147.4, 154.3 (t, J = 3.6 Hz), 192.3. $^{31}P\{^1H\}$ NMR (162 MHz, DMSO-d6) δ, ppm: 8.5 (d, J = 94.1 Hz), 24.3 (dd, J = 95.8, 92.6 Hz). ESI-TOF HRMS: [M] 804.1075 (calcd 804.1066)

2-Amino-substituted acetohydrazone-terminated biphenyl-blocked dendrimers

Aldehyde-terminated biphenyl-blocked dendrimer (**6**) (0.25 mmol) was dissolved in 10 mL $CHCl_3$, then solution of an acetohydrazide (1.025 mmol) in 10 mL methanol was added. Reaction mixture was acidified to pH~5 with acetic acid and stirred overnight at r.t. Once the completeness of aldehyde conversion into hydrazone was confirmed by ^1H NMR, the solvent was removed, and the solid residue was washed with $CHCl_3$ and diethyl ether, then dried.

Pyridinium-terminated dendrimer PG0L

Pale powder, yield: 90%. ^1H NMR (400 MHz, DMSO-d6) δ, ppm: 5.69, 6.11 (2d, J = 7.7 Hz, 8H, C(O)-CH_2-N), 6.86 (t, J = 8.9 Hz, 2H, biphenyl), 7.21 (m, 8H, CH-C-CH=N), 7.48 (m, 4H, biphenyl), 7.66 – 7.86 (m, 10H, O-C-CH, biphenyl), 8.22 (q, J = 9.6, 8.1 Hz, 8H, pyridinium), 8.30 - 8.52 (m, 4H, CH=N), 8.69 (q, J = 6.4, 4.9 Hz, 4H, pyridinium), 9.08 – 9.19 (m, 8H,

pyridinium), 12.43, 13.21 (2m, N-NH). $^{13}C\{^{1}H\}$ NMR (101 MHz, DMSO-d6) δ, ppm: 61.39, 61.83, 121.72 (d, J = 20.9 Hz), 127.28, 127.85 – 128.35 (m), 129.24 (d, J = 16.7 Hz), 130.66 (d, J = 30.4 Hz), 131.86, 144.58, 146.76 (d, J = 10.8 Hz), 146.99, 147.47 (d, J = 11.5 Hz), 151.44, 161.86, 166.96 (d, J = 13.9 Hz), 172.44.$^{31}P\{^{1}H\}$ NMR (162 MHz, DMSO-d6) δ, ppm: 9.1 (dd, J = 93.4, 7.2 Hz), 24.8 (dd, J = 94.8, 91.7 Hz). ESI-TOF HRMS: $[M]^{2+}$ 668.6871 (calcd 668.6852), $[M]^{3+}$ 446.1274 (calcd 446.1261), $[M]^{4+}$ 334.8477 (calcd 334.8465).

Trimethylammonium-terminated dendrimer TG0L

Pale powder, yield: 99%. ^{1}H NMR (400 MHz, DMSO-d6) δ, ppm: 3.39 (s, 36H, N-CH_3), 4.46, 4.86 (2d, J = 11.6 Hz, 8H, C(O)-CH_2-N), 6.91 (dd, J = 53.4, 7.9 Hz, 2H, biphenyl), 7.18 (m, 8H, <u>CH</u>-C-CH=N), 7.43 – 7.58 (m, 4H, biphenyl), 7.64 – 7.80 (m, 10H, O-C-<u>CH</u>, biphenyl), 8.19 – 8.50 (m, 4H, CH=N), 12.12 – 12.54, 12.96 – 13.30 (2m, 4H, N-NH). $^{13}C\{^{1}H\}$ NMR (101 MHz, DMSO-d6) δ, ppm: 53.50 – 54.16 (m), 62.65 (d, J = 9.3 Hz), 63.83, 121.01 – 122.09 (m), 127.27, 128.21, 129.13 – 129.62 (m), 130.50, 130.85 (d, J = 9.4 Hz), 131.44 – 131.90 (m), 144.81 (d, J = 13.8 Hz), 147.44 (d, J = 9.6 Hz), 148.13 (d, J = 11.4 Hz), 151.50 (d, J = 16.5 Hz), 160.41 (d, J = 6.3 Hz), 162.59 (d, J = 21.0 Hz), 165.79 (d, J = 15.3 Hz). $^{31}P\{^{1}H\}$ NMR (162 MHz, DMSO-d6) δ, ppm: 9.0 (d, J = 93.7 Hz), 24.6 (m). ESI-TOF HRMS: $[M]^{2+}$ 628.7490 (calcd 628.7478), $[M]^{3+}$ 419.5015 (calcd 419.5011), $[M]^{4+}$ 314.8788 (calcd 314.8778).

Triethylammonium-terminated dendrimer NEt_3G0L

Pale powder, yield: 90%. ^{1}H NMR (400 MHz, DMSO-d6) δ, ppm: 1.27 (dt, J = 20.6, 7.1 Hz, 36H, N-CH_2-<u>CH_3</u>), 3.52, 3.61 (2d, J = 7.5 Hz, 24H, N-<u>CH_2</u>-CH_3), 4.35, 4.60 (2m, 8H, C(O)-CH_2-N), 6.85 (m, 2H, biphenyl), 7.21 (m, 8H, <u>CH</u>-C-CH=N), 7.46 (p, J = 7.3 Hz, 4H, biphenyl), 7.63 – 7.78 (m, 8H, O-C-<u>CH</u>), 7.84 (m, 2H, biphenyl), 8.25, 8.46 (2m, 4H, CH=N), 12.28 ,13.44 (2m, 4H, N-NH). $^{13}C\{^{1}H\}$ NMR (101 MHz, DMSO-d6) δ, ppm: 8.02 (d, J = 2.1 Hz), 53.39 – 56.32 (m), 121.68 (d, J = 27.0 Hz), 127.25, 128.19, 129.48 (d, J = 8.4 Hz), 130.64 (d, J = 27.1 Hz), 131.68 (d, J = 7.5 Hz), 144.94, 147.44 (d, J = 9.5 Hz), 148.20 (d, J = 13.3 Hz), 151.61, 160.14, 162.16, 165.52. $^{31}P\{^{1}H\}$ NMR (162 MHz, DMSO-d6) δ, ppm: 8.9 (m), 24.6 (m). ESI-TOF HRMS: $[M]^{2+}$ 712.8425 (calcd 712.8417), $[M]^{3+}$ 475.5643 (calcd 475.5638), $[M]^{4+}$ 356.9242 (calcd 356.9248).

1-methyl-piperidinium-terminated dendrimer C6MeG0L

Pale powder, yield: 90%. ^{1}H NMR (400 MHz, DMSO-d6) δ, ppm: 1.56 (m, 8H, N-CH_2-CH_2-<u>CH_2</u>-), 1.87 (m, 16H, N-CH_2-<u>CH_2</u>-), 3.35 (s, 12H, CH_3-N), 3.37 – 3.81 (m, 16H, N-<u>CH_2</u>-CH_2-), 4.54, 4.83 (2d, J = 5.3 Hz, 8H, C(O)-<u>CH_2</u>-N), 6.87 (m, 2H, biphenyl), 7.20 (m, 8H, <u>CH</u>-C-CH=N), 7.47 (m, 4H, biphenyl), 7.73 (m, 10H, O-C-<u>CH</u>, biphenyl), 8.19 – 8.51 (m, 4H, CH=N),

12.32, 13.31 (2m, 4H, N-NH).$^{13}C\{^{1}H\}$ NMR (101 MHz, DMSO-d6) δ, ppm: 19.85 (d, J = 3.0 Hz), 20.94 – 21.33 (m), 47.45, 47.87, 50.43, 60.10, 61.52 – 62.18 (m), 121.60 (q, J = 16.1, 13.3 Hz), 127.26, 128.20, 129.43 (d, J = 6.7 Hz), 130.65 (d, J = 30.6 Hz), 131.67 (d, J = 5.7 Hz), 144.79 (d, J = 10.1 Hz), 147.44 (d, J = 9.2 Hz), 148.21 (d, J = 10.8 Hz), 151.53 (d, J = 16.0 Hz). $^{31}P\{^{1}H\}$ NMR (162 MHz, DMSO-d6) δ, ppm: 9.0 (m), 24.7 (m).ESI-TOF HRMS: $[M]^{2+}$ 708.8105 (calcd 708.8104), $[M]^{3+}$ 472.8761 (calcd 472.8762), $[M]^{4+}$ 354.9090 (calcd 354.9091).

1-methyl-pyrrolidinium-terminated dendrimer C5MeG0L

Pale powder, yield: 90%. ^{1}H NMR (400 MHz, DMSO-d6) δ, ppm: 2.13 (m, 16H, N-CH_2-$\underline{CH_2}$-), 3.36 (s, 12H, CH_3-N), 3.75 (m, 16H, N-$\underline{CH_2}$-CH_2-), 4.48, 4.91 (2d, J = 6.4 Hz, 8H, C(O)-$\underline{CH_2}$-N), 6.88 (m, 2H, biphenyl), 7.20 (m, 8H, $\underline{CH}$-C-CH=N), 7.48 (m, 4H, biphenyl), 7.72 (m, 10H, O-C-$\underline{CH}$, biphenyl), 8.16 – 8.50 (m, 4H, CH=N), 12.31, 13.21 (2m, 4H, N-NH). $^{13}C\{^{1}H\}$ NMR (101 MHz, DMSO-d6) δ, ppm: 20.48 – 22.99 (m), 48.28 – 50.45 (m), 62.24 (d, J = 22.5 Hz), 65.37, 121.04 – 122.18 (m), 127.28, 128.21, 129.36 (d, J = 12.4 Hz), 130.66 (d, J = 30.6 Hz), 131.64, 144.63 (d, J = 9.8 Hz), 147.45 (d, J = 9.4 Hz), 148.03 (d, J = 11.6 Hz), 151.50 (d, J = 15.0 Hz), 160.70, 165.88 – 166.54 (m). $^{31}P\{^{1}H\}$ NMR (162 MHz, DMSO-d6) δ, ppm: 9.0 (d, J = 93.2 Hz), 24.7 (m). ESI-TOF HRMS: $[M]^{2+}$ 680.7794 (calcd 680.7791), $[M]^{3+}$ 454.1890 (calcd 454.1887), $[M]^{4+}$ 340.8929 (calcd 340.8935).

*Piperidinyl-terminated dendrimer*C6HG0L

Pale powder, yield: 80%. ^{1}H NMR (400 MHz, DMSO-d6) δ, ppm: 1.41 (m, 8H, N-CH_2-CH_2-$\underline{CH_2}$-), 1.55 (q, J = 5.7 Hz, 16H, N-CH_2-$\underline{CH_2}$-), 2.43 (d, J = 5.9 Hz, 16H, N-$\underline{CH_2}$-CH_2-), 3.04, 3.36 (2m, 8H, C(O)-CH_2-N), 6.78 (m, 2H, biphenyl), 7.18 (m, 8H, $\underline{CH}$-C-CH=N), 7.44 (m, 4H, biphenyl), 7.68 (m, 10H, O-C-$\underline{CH}$, biphenyl), 7.84 – 8.43 (m, 4H, CH=N), 11.20 (m, 4H, N-NH). $^{13}C\{^{1}H\}$ NMR (101 MHz, DMSO-d6) δ, ppm: 21.54, 24.09 (d, J = 14.8 Hz), 25.91 (d, J = 17.6 Hz), 54.51 (d, J = 26.1 Hz), 58.40, 61.94, 121.71 (d, J = 23.9 Hz), 127.15, 128.21, 128.73, 129.12, 130.53 (d, J = 21.2 Hz), 132.37, 141.95 (d, J = 19.1 Hz), 146.54 (d, J = 14.1 Hz), 147.47 (d, J = 9.3 Hz), 151.15 (d, J = 21.1 Hz), 166.57, 171.35, 172.44 (d, J = 6.8 Hz). $^{31}P\{^{1}H\}$ NMR (162 MHz, DMSO-d6) δ, ppm: 9.2 (dt, J = 94.6, 11.1 Hz), 24.9 (m). ESI-TOF HRMS: $[M+2H]^{2+}$ 680.7798 (calcd 680.7800), $[M+3H]^{3+}$ 454.1888 (calcd 454.1887), $[M+4H]^{4+}$ 340.8928 (calcd 340.8935).

Bacterial Strains

All the dendrimers synthesized were primarily screened by following Clinical and Laboratory Standard Institute (CLSI) guidelines[20] against *E. coli* ATCC 25922, *S. aureus* ATCC 29213, *K. pneumoniae* BAA 1705, *A. baumannii* BAA 1605, *P. aeruginosa* ATCC 27853, *Enterobacter* sp and *Enterococcus spp.*, collectively known as ESKAPE pathogens. The screening

includes the drug-resistant clinical strains of *S. aureus* and *Enterococcus* spp, including those resistant to vancomycin and other clinically utilized antibiotics. These strains were procured from Biodefense and Emerging Infections Research Resources Repository/Network on Antimicrobial Resistance in *Staphylococcus aureus*/American Type Culture Collection (BEI/NARSA/ATCC, USA) and routinely cultivated on MHA and MHBII. To obtain the starter culture, a single colony was picked from the MHA plate, inoculated in MHBII, and incubated overnight at 37°C with shaking for 18–24h.

Growth media and reagents

All bacterial media and supplements, including Cation supplemented Mueller–Hinton broth II (MHBII), Mueller–Hinton agar (MHA) and tryptic soy broth (TSB) were purchased from Becton-Dickinson (Franklin Lakes, NJ, USA). All other chemicals and antibiotics were procured from Sigma-Aldrich (St. Louis, MO, USA). While performing the experiments, all the relevant guidelines and regulations were followed.

Antibiotic susceptibility testing

CLSI guidelines for microdilution assay were followed to conduct the antibiotic susceptibility testing[20]. 10 mg/ml stock solution of tested compounds were prepared in dimethyl sulfoxide (DMSO)/water. MHBII was used to inoculate bacterial culture, and optical density (OD) was measured at 600 nm, followed by dilution to achieve ~10^5 colony-forming units (CFU)/mL. The compounds were tested from 64 to 0.5 µg/mL in a two-fold serial diluted fashion, with 2.5 µL of each concentration added to the wells of a 96-well round-bottomed microtiter plate. Later,97.5 µL of bacterial suspension was added to each well containing either the test compound or appropriate control. The plates were incubated at 37 °C for 18-24 h, and minimum inhibitory concentration (MIC) was determined. The MIC is defined as the lowest concentration of the test compounds at which no visible growth was observed. MIC determination for each test compound was carried out independently three times using duplicate samples.

PMBN Assay

Polymyxin B nonapeptide (PMBN) is a derivative of Polymyxin B, that lacks direct bactericidal activity but increases outer membrane (OM) permeabilization, thus permitting increased entry of xenobiotics in GNB[21, 22]. Previous studies were followed to determine the MIC of antimicrobials in the presence of PMBN[22]. The MIC of AE4G0, vancomycin, Levofloxacin and rifampicin were determined against *E. coli* ATCC 25922 and *A. baumannii* BAA 1605 in the presence of PMBN at a concentration of 10 µg/ml.

Cytotoxicity against Vero cells (ATCC CCL-81)

The cytotoxicity of all synthesized dendrimers were checked against eukaryotic Vero cells using MTT assay, CC_{50} was determined and the selectivity index was calculated[23]. Doxorubicin was used as a positive control and each experiment was repeated in triplicate.

Bacterial time-kill kinetics

Time kill kinetics was used to assess the bactericidal activity of the AE4G0[24, 25]. Briefly, *S. aureus* ATCC 29213 was diluted ~10^5 CFU/mL in MHBII, treated with 1x and 10x MIC of AE4G0 and vancomycin and incubated at 37°C with shaking for 24 h. 100 µL samples were collected at 0 h, 1 h, 6 h and 24 h, serially diluted in PBS and plated on MHA, followed by incubation at 37 °C for 18–20 h. Time-kill curves were constructed by counting the colonies from plates and plotting the CFU/mL of surviving bacteria at each time point in the presence and absence of the compound. Each experiment was repeated three times in duplicate, and the mean data were plotted.

Drug Interaction with FDA-approved drugs

Interaction of AE4G0 with standard drugs approved by FDA was determined by chequerboard method[26]. As recommended by CLSI, serial two-fold dilutions of each drug were prepared before testing. AE4G0 was diluted two-fold along ordinate ranging from 64 to 0.5 µg/mL (8 dilutions). In contrast, antibiotics were serially diluted (twelve dilutions), ranging from 64-0.03 µg/mL for ceftazidime, 4–0.0019 µg/mL for daptomycin and vancomycin, 2-0.0009 µg/mL for levofloxacin, gentamicin, minocycline and meropenem, 0.06-0.000014 µg/mL for rifampicin and 16-0.0078 µg/mL for linezolid in 96-well microtiter plates. Ninety-five microlitres of ~10^5 CFU/mL were added to each well and plates were incubated at 37^0C for 18-24 h. After incubation, FICs (fractional inhibitory concentrations) were calculated as follows: ∑FIC = FIC A + FIC B, where FIC A is MIC of Drug A in combination/MIC of Drug A alone and FIC B is MIC of Drug B in combination/MIC of Drug B alone. The combination is synergistic when ∑FIC is ≤0.5, indifferent when ∑FIC is >0.5 to 4, and antagonistic when ∑FIC is >4[26].

AE4G0 activity against pre-formed *S. aureus* biofilm

Antibiofilm activity of AE4G0 was determined as described previously[27]. Briefly, in 1% TSB, *S. aureus* ATCC 29213 was cultured overnight at 37°C and 180 rpm. The overnight culture was diluted at 1:100 in TSB supplemented with 1%

glucose and 0.2 mL/well was transferred into 96-well polystyrene flat-bottom tissue culture plates. To increase biofilm formation, low oxygen concentration was maintained and kept at 37^0C for 48h. Post-incubation media were decanted, and plates were rinsed gently three times with 1xPBS (pH=7.4) to remove the planktonic bacteria. Plates were refilled with TSB with different drug concentrations and incubated for 24 h at 37^0C. After drug treatment, the media was decanted, washed three times with 1x PBS (pH 7.4), and biofilm was fixed by incubating the plate at 60^0C for 1 h. After fixing, the biofilm is stained with 0.06% crystal violet for 10 min, rinsed with PBS, and dried at room temperature. The bound crystal violet was eluted with 30% acetic acid (0.2 mL) for biofilm quantification. Absorbance was taken on a microtiter plate reader at 600 nm for biofilm quantification.

Determination of post-antibiotic effect (PAE)

Post antibiotic effect (PAE) of AE4G0 was determined as reporte earlier[28]. Overnight culture of *S. aureus* ATCC 29213 was diluted in MHBII ~10^5 CFU/mL, exposed to 1x MIC and 10x MIC of AE4G0 and vancomycin and incubated at 37 °C for 1 h. Following incubation, the culture was centrifuged and washed twice with pre-warmed MHBII to remove any traces of antibiotics. Finally, cells were resuspended in drug-free MHBII and incubated further at 37°C. Samples were taken every 1 h, serially diluted, and plated on TSA for enumeration of CFU. PAE was calculated as PAE = T – C, where T is the difference in time required for 1 $\log_{10}$ increase in CFU vs. CFU observed immediately after removing the drug and C in a similarly treated drug-free control.

Induction of resistance in *S. aureus* ATCC 29213 against AE4G0

The emergence of resistant bacteria to AE4G0 was assessed, and the frequency of resistant mutants was evaluated by serial exposure of the organism to an antimicrobial agent[29]. *S. aureus* ATCC 29213 was exposed to serial passage of AE4G0 and Levofloxacin and monitored for changes in MIC for 35 days, following which antibiogram was determined.

Scanning Electron Microscopy with AE4G0 against *S. aureus* ATCC 29213

Scanning Electron Microscopy (SEM) was utilized to determine any compound-induced topological changes in *S. aureus* ATCC 29213 following treatment with AE4G0. The mid-log phase grown bacteria (10^8 cfu/mL) were treated with 10x MIC of AE4G0 for 1 h, whereas untreated control was treated with vehicle control DMSO and processed in the same manner. After treatment, the cells were washed twice with phosphate buffer saline (PBS) pH 7.2. Subsequently, cells

were fixed in aldehyde fixative 2% glutaraldehyde and 4% paraformaldehyde in PBS pH 7.2 overnight. The cells were adhered on poly-L-lysine coated glass coverslips and osmicated in 1% OsO_4. Then the cells were gradually dehydrated in an ascending graded series of ethanol, critical point dried, and sputter coated with Au-Pd (80:20) using a Polaron E5000 sputter coater. Bacterial morphology was examined in an FEI Quanta 250 SEM using an SE detector at an accelerating voltage of 30 kV.

Fluorescence Microscopy with AE4G0 against *S. aureus* ATCC 29213

S. aureus viability in the presence of AE4G0 was evaluated using the LIVE/DEAD *BacLight* bacterial viability kit (Invitrogen, catalogue no. L7007). *S. aureus* ATCC 29213 cells were grown to an OD_{600} 0.2 were treated with AE4G0 at 1x and 10x MIC for 1 h. After incubation, cells were washed three times and resuspended in saline. 3 µl of SYTO9 and PI (mixed in equal volumes) provided in the kit were added to each sample with the final volume of 1 ml and incubated at room temperature in the dark for 15 minutes. Fluorescent images of stained bacteria were obtained using a Fluorescence microscope (EVOS FLc). The Emission/Excitation wavelength for Syto9 is 485/498, whereas for PI Emission/Excitation wavelength was 535/617 nm.

Murine skin infection model

The *in vivo* potential of AE4G0 to eliminate *S. aureus* infection was determined by following the superficial skin infection model and experiments were performed as described previously with slight modifications[30]. Briefly, male swiss mice 4-6 weeks old, weighing ~22–24 g, were used throughout the study and were caged alone in an Individually vented cage (IVC) to check cross-contamination and to maintain aseptic conditions throughout the experiment. Ketamine and xylazine were prepared in distilled water 40mg/kg and 8mg/kg of body weight, respectively, and injected intraperitoneally (IP) as a mixture of 100 µl in each mouse for anaesthesia. Then, we proceeded with the removal of fur by applying depilatory cream; the area was cleaned with the help of sterile distilled water. Approximately, 2 cm^2 of skin area was scratched till it became visibly damaged and was characterized by reddening and glistening without any bleeding. For bacterial infection, a 10 µl droplet containing 10^7 CFU/mL of *S. aureus* ATCC 29213 and/or gentamicin-resistant MRSA NRS119 was applied to the reddened area of skin. To confirm the infection, post 4 h, untreated mice were sacrificed. Various dilutions were plated on TSA plate at the exact time dosing of the treatment groups, i.e., 2%

fusidic acid (positive control), 1% AE4G0, and untreated (vehicle) was started, followed by a second dose post 16 hours from the first dose and henceforth, drug regimen comprised of twice daily application (in the morning and the evening, with an 8 h interval) for 4 days. The mice were treated with 25-30 mg of each-2% Fusidic acid (LEO Pharma, Ballerup, Denmark), 1% AE4G0 and untreated (vehicle) regularly. All groups were sacrificed post 18 h of the last dose to avoid the carryover effects of the treatment group. Around ~2 cm^2 of wounded skin post sacrifice were excised and homogenized with 500 µl phosphate-buffered saline (1x PBS) in 2ml MP tissue grinding Lysing Matrix F tubes using MP FastPrep®-24 set at 4.0 M/S for 30 s (3 cycles). The dilutions were plated post-homogenization on TSA plates, followed by overnight incubation at 37°C to determine the bacterial CFU count in each treatment group. Each experiment was repeated three times in duplicate and the mean and SEM of Log_{10} CFU/gm were plotted.

Ethics approval

Animal experiments were performed on six-eight-week-old swiss mice procured from the National Laboratory Animal Facility of CSIR-Central Drug Research Institute, Lucknow. The experimental protocols were reviewed and approved by the Institutional Animal Ethics Committee of CSIR-Central Drug Research Institute, Lucknow (IAEC/2019/2/Renew-1/ Dated-22.06.2020). Animal experiments were performed per the guidelines provided by the Committee for Control and Supervision of Experiments on Animals (CPCSEA, Govt. of India)

Statistical analysis

Statistical analysis was performed using GraphPad Prism 8.0.2 software (GraphPad Software, La Jolla, CA, USA). Comparison between three or more groups was analyzed using a one-way analysis of variance with Dunnett's multiple comparison test. P-values<0.0001 were considered to indicate significance.

Results and discussion

Synthesis of cationic dendrimer species

Cationic acetohydrazides are considered useful tools for functionalizing surfaces to produce devices for biomedical use. In particular, ammonium and pyridinium acetohydrazides (so-called Girard reagents T and P) have found wide use. Remarkably, when grafted onto dendrimer scaffolds, acetohydrazides bring new modalities to the macromolecules. For example, phosphorus dendrimers bearing Girard T, P moieties (as acetohydrazones) on the surface are able to form single-component, physical hydrogels through the interdigitation of dendrimer branches stabilized by hydrogen

bonding between hydrazone fragments on the surface[17, 31-33]. Furthermore, acetohydrazone-functionalized dendrimers help to modulate the rate of drug release from macroscale biomaterials. In view of this, it is interesting to assess the biological activity of acetohydrazone-terminated phosphorus dendrimers. The series of cationic acetohydrazides **(3a-g)** differing by structure of a cation were synthesized in high yields, based on the methyl chloroacetate by sequential substitution of chlorine with different amines to form cationic esters **(2a-g)** followed by hydrazinolysis of an ester bond. (Scheme 1)

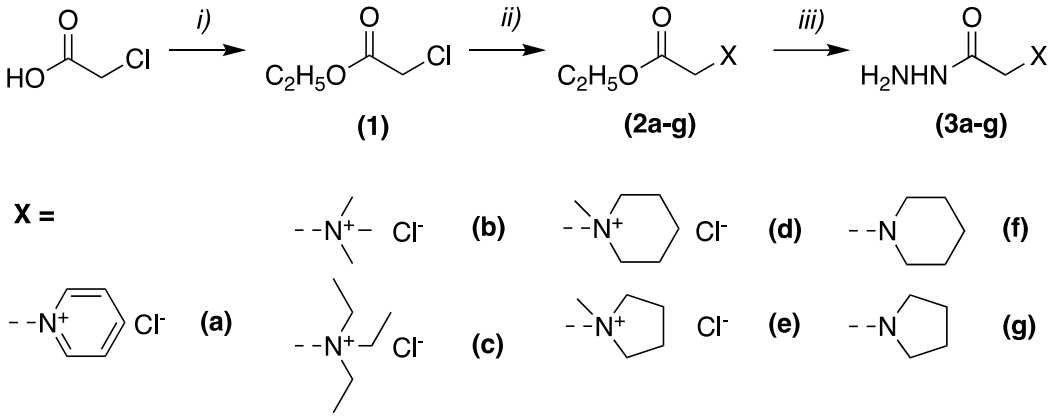

Scheme 1: Synthesis of cationic acetyhydrazides **3a-g** Conditions: *i)* HCl, ethanol; *ii)* amine, CH_3CN, 90 ˚C; *iii)* N_2H_4, methanol, 90˚C, 60-95%.

The dendritic scaffold used was either hexafunctional (hexa(hydroxybenzaldehyde) cyclotriphosphazene) or tetrafunctional one (*P,P*-dihydroxybiphenyl-*P',P',P'',P''*-tetra (hydroxybenzaldehyde) cyclotriphosphazene). The functionalization of dendrimer surface with cationic moieties was done by a simple reaction between acetohydrazides and aldehyde-terminated dendrimers upon acidic catalysis to form corresponding acetohydrazones (Scheme 2). The completeness of conversion was monitored by the disappearance of aldehyde signal in ^{1}H NMR spectra. The resulting products (see Fig 1) were obtained in high yields. In the case of dendrimer species bearing tertiary amines, the protonation with HCl was done at the last stage.

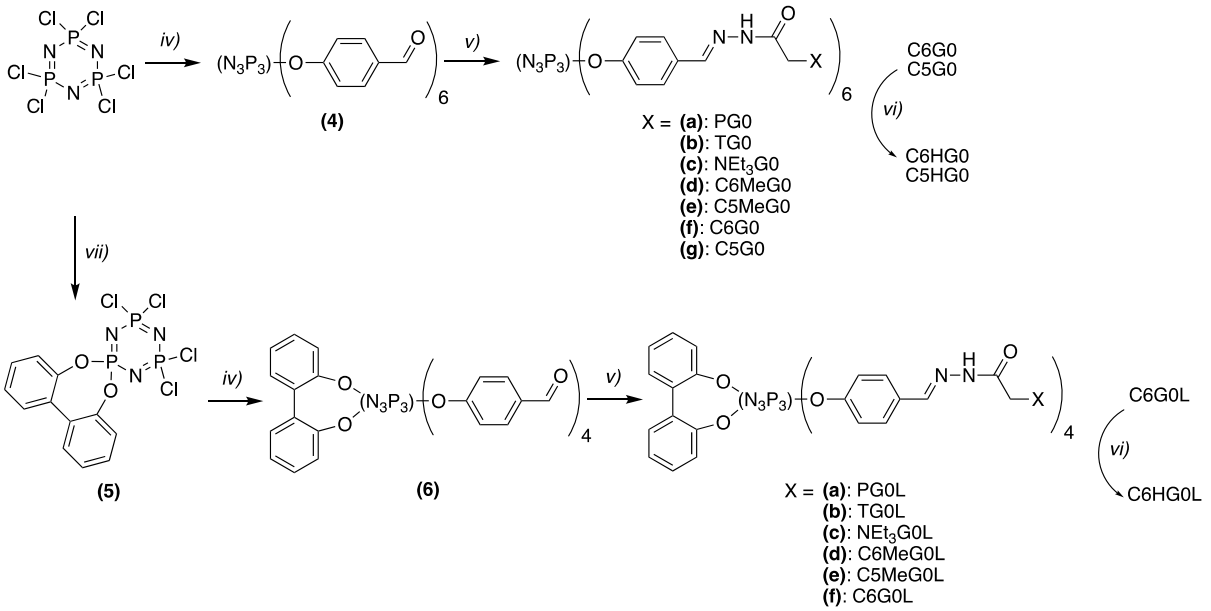

Scheme 2: Synthesis of the cationic phosphorus dendrimers generation 0. Conditions: *iv)* 4-hydroxybenzaldehyde, CH_3CN, K_2CO_3, 92%; *v)* (**3a-g**), $CHCl_3$:methanol (1:1), acetic acid to pH~5, 85+%; vi) HCl/diethyl ether, THF, 0 ˚C; vii) 2,2'-dihydroxybiphenyl, CH_3CN, K_2CO_3.

Fig 1: Structures of various dendrimers synthesized and tested.

Dendrimer	Structure	Dendrimer	Structure
AE4G0	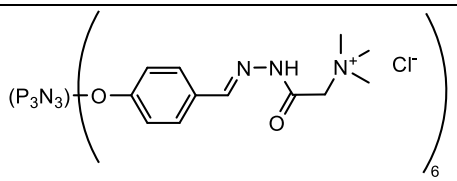	PG0L	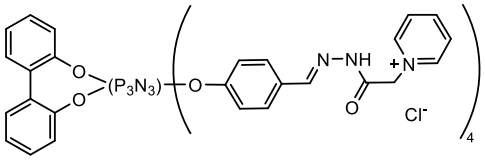
PG0	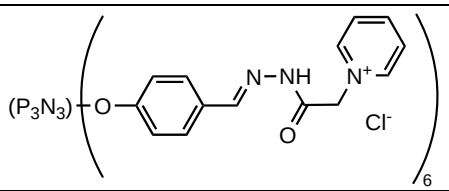	TG0L	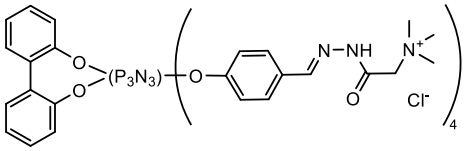
NEt3G0	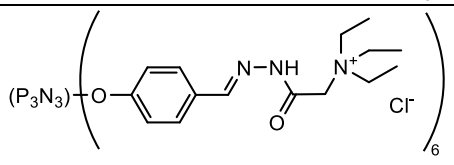	NEt3G0L	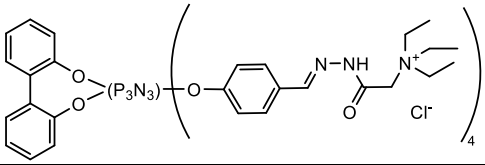
C5HG0	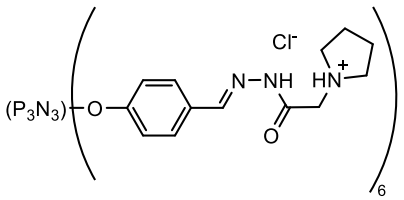	C6HG0L	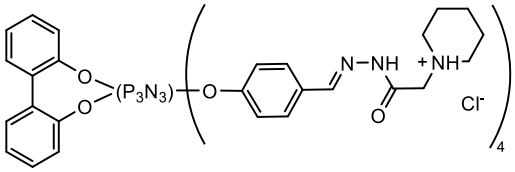
C6HG0	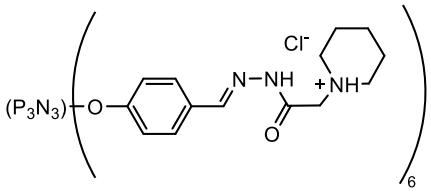	C5MeG0L	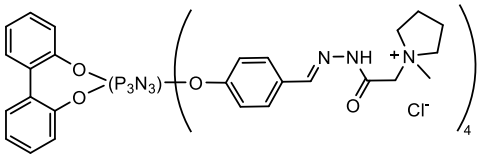

C5MeG0	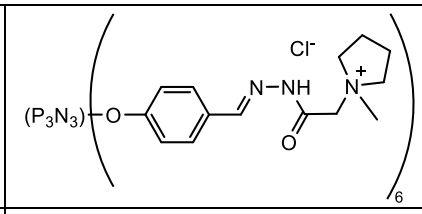	C6MeG0L	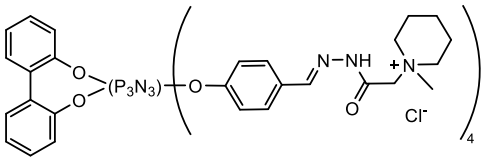
C6MeG0	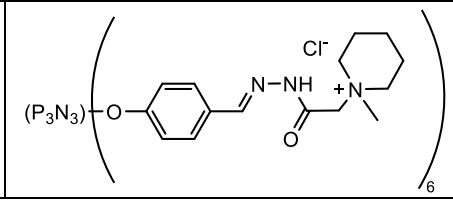		

385

386

387 **AE4G0 is potently active against *S. aureus* ATCC 29213 and *Enterococcus* sp**

388 After synthesis and purification, the antimicrobial activity of the synthesized low-generation phosphorus dendrimers
389 was determiend against bacterial pathogen panel (S2 SI). As seen, except for piperidinyl-terminated dendrimers, all
390 other low-generation dendrimers were active against gram-positive *S. aureus* ATCC 29213 (MIC 4-32 mg/L). PG0L and
391 C5HG0 were active against GNB but at higher MIC 16-64 mg/L (S2 SI). From all these, AE4G0 was selected to be
392 screened further due to its low MIC against *S. aureus,* i.e., 4-8 mg/L coupled with ease of synthesis of AE4G0 and more
393 eco friendly. On the other hand, AE4G0 is inactive against GNB including *E. coli, A. baumannii, K. pneumoniae* and *P.*
394 *aeruginosa* (Table 1).
395 Furthermore, AE4G0's antibacterial property was tested against clinical drug-resistant strains of *S. aureus* and
396 *Enterococcus* sp, including MRSA and VRSA, where it showed almost equipotent activity against all the tested strains,
397 irrespective of their resistance mechanism, suggesting a new mechanism of action and lack of cross-resistance with
398 existing drugs.

399

400 **PMBN does not influence the entry of AE4G0 into GNB pathogens**

401 Typically, the OM of GNB presents a very significant barrier to the entry of antibiotics, thus PMBN, a delipidated version
402 of polymyxin B is utilized as reagent to study the entry of molecules under investigation into GNB. As seen in S3(SI),
403 vancomycin and rifampicin MIC decreased by several folds in the presence of PMBN as expected whereas no change in
404 MIC was observed for AE4G0, against *E. coli* ATCC 25922 and *A. baumannii* BAA 1605 (S3 SI), suggesting that intact OM
405 of GNB has negligible impact on AE4G0 activity against GNB pathogens.

406

AE4G0 is not cytotoxic against eukaryotic Vero cells

When tested for cytotoxicity against Vero cells, AE4G0 demonstrated CC_{50} of >250 mg/L, which gives a selectivity index of >31.25 (Table 2). This very good selectivity index of AE4G0 supported taking it further for pre-clinical development.

AE4G0 exhibits concentration-dependent time-kill kinetics against *S. aureus* ATCC 29213

Time kill kinetics are a very important parameter to determine the efficacy of a compound under investigation. In this context, the bacterial time-kill kinetics of AE4G0 were assessed at 1x and 10x MIC along with vancomycin as control against *S. aureus* ATCC 29213 and the results are plotted in Fig 2a. At 10x MIC in 24 h, AE4G0 reduced >7 log_{10} CFU/mL as compared to untreated *S. aureus* ATCC 29213, which is comparable to vancomycin. Thus, AE4G0 exhibits concentration-dependent, bactericidal activity against *S. aureus* ATCC 29213 which is comparable to vancomycin.

AE4G0 synergizes with gentamicin against *S. aureus* ATCC 29213 and gentamicin-resistant MRSA NRS119

Drug-combinations are an integral part of treatment plans for many infectious diseases; thus the combination potential of any new investigational molecule is determination with approved FDA drugs. Thus, AE4G0 was tested for synergy with FDA-approved drugs such as daptomycin, ceftazidime, linezolid, gentamicin, levofloxacin, meropenem, minocycline, rifampicin and vancomycin using chequerboard method as seen in Table 3. As can be seen, AE4G0 partially synergized with gentamicin against *S. aureus* ATCC 29213[34], which was further confirmed using time-kill analysis using both compounds at 1x MIC. As seen in Fig 2b, combination of AE4G0 and gentamicin demonstrate a reduction of >2 log_{10} CFU/mL of bacterial load compared with initial inoculam at 24h, also in combination it reduces the bacterial load >2 log_{10} CFU/mL compared with the most potent drug alone i.e.AE4G0 alone, which is the criteria for synergy in time -kill kinetics[35, 36]. Next, the effect of the combination was tested against gentamicin-resistant MRSA NRS119, and AE4G0 partially synergises with gentamicin as it reduced the bacterial load >1 log10 CFU/mL compared with initial inoculum at 24h, in combination it reduces bacterial load ~1 log10 CFU/mL compared with the most potent drug alone i.e. AE4GO , Interestingly in combination it reduces the bacterial load ~6.0 log_{10} CFU/mL compared with untreated at 24h, AE4GO in combination with gentamicin significantly better than either drug alone (Fig 2c). Thus, taken together chequerboard method and time kill-kinetics assay, AE4G0 combines spectacularly with gentamicin against *S. aureus* ATCC 29213 and partially synergizes against gentamicin-resistant MRSA NRS119 and exhibits superior killing kinetics a compared to individual drugs.

AE4G0 annihilates pre-formed *S. aureus* biofilm

Bacteria under stressful conditions make biofilms to negate the action of xenobiotic molecules, including antibiotics, often leading to recurrent infections and consequently, therapeutic failure. As a consequence, many FDA-approved antibiotics demonstrate limited activity against bacterial biofilms, so we investigated the activity of AE4G0 against pre-formed *S. aureus* biofilms along with vancomycin and levofloxacin. As seen in Fig 3, AE4G0 eradicates biofilm significantly better than levofloxacin and vancomycin at 1x MIC. Thus, AE4G0 exhibits potent activity against bacteria under in different physiological conditions, which is an essential part of an antimicrobial, as stated earlier[16].

AE4G0 exhibits a prolonged Post antibiotic effect (PAE)

PAE is an important pharmacokinetic parameter that influences the dosing regimen as well as the emergence of resistance; thus, it is an important parameter to be determined in pre-clinical assessment. The PAE of AE4G0 was determined along with vancomycin against *S. aureus* ATCC 29213. As seen in Table 4, AE4G0 exhibits a PAE of ~15.5 h, which is much more than that of vancomycin, thus exhibiting an essential characteristic distinguishing it from vancomycin. All combined, AE4G0 exhibits concentration-dependent bactericidal activity with long PAE.

AE4G0 does not induce resistance in *S. aureus* ATCC 29213.

Emergence of resistance is inevitable to any molecule in clinical use, thus the frequency of resistance of AE4G0 was determined by serial exposure to *S. aureus* ATCC 29213 over 35 days along with levofloxacin and the MIC is plotted in Fig 4. As seen, despite consistent exposure, AE4G0 fails to induce resistance in *S. aureus* ATCC 29213, whereas, under the same conditions, *S. aureus* generates stable, high resistance to levofloxacin. Antibiogram of *S.aureus* ATCC 29213 grown in presence of AE4G0 for 35 passages does not shows cross-resistance to approved antibiotics can be seen in S4 (SI). Thus, AE4G0 exhibits concentration dependent bactericidal kinetics with long PAE and does not induce resistance in *S. aureus*.

AE4G0 causes cellular lysis of *S. aureus* ATCC 29213 as seen by Fluorescence and Scanning electron microscopy (SEM)

To decipher the mechanism of action of AE4G0 on *S. aureus*, AE4G0 treated *S. aureus* were stained with LIVE/DEAD *Bac*Light bacterial viability kit (Invitrogen, catalog no. L7007) as per manufacturer's instructions and visualized by Fluorescence microscopy using EVOS FLc microscope using 100x oil immersion objective. As visualized in Fig 5,

treatment with 10x MIC of AE4G0 for 1 h led to dead bacterial cells (stained red) compared to untreated viable cells (stained green).

This cellular destruction was further probed by visualizing the samples treated with 10x MIC of AE4G0 for 1 h with scanning electron microscopy (SEM) at 30,000x magnification, and the results are shown in Fig 5. As compared to untreated cells, widespread cell destruction is visible in AE4G0-treated *S. aureus* cells, with lots of intracellular debris oozing out from lysed cells. Together, these results clearly demonstrate the cellular disruption of *S. aureus* ATCC 29213 upon treatment with AE4G0.

AE4G0 exhibits potent *in vivo* activity in murine skin model

Since *in vitro* AE4G0 exhibits promising antimicrobial activity against clinical drug-resistant isolates of *S. aureus*, its *in vivo* activity against *S. aureus* ATCC 29213 was determined in a murine skin infection model. AE4G0 demonstrated ~1.2 $\log_{10}$ CFU/gm reduction in bacterial load compared to untreated, while fusidic acid reduced ~2.5 $\log_{10}$ CFU/gm compared to untreated. Statistical analysis upholds the significance ($p<0.0001$) of the AE4G0 efficacy in reducing bacterial load in skin infection mode, as seen in Fig 6a. In addition, when the combination of AE4G0 and gentamicin was tested against gentamicin-resistant MRSA NRS119, combination was more efficacious than either drug alone and reduced ~0.7 $\log_{10}$ CFU/gm ($p<0.01$) as compared to untreated, whereas AE4G0 reduced ~0.55 $\log_{10}$ CFU/gm alone while gentamicin reduced ~0.3 $\log_{10}$ CFU/gm, thus further demonstrating the power of the combination against drug-resistant *S. aureus* (Fig 6b). All combined, the potent *in vitro* activity of AE4G0 is exquisitely translated *in vivo* as well alone and in combination with gentamicin.

All combined, AE4G0 is a novel, phosphorus dendrimer exhibiting direct equipotent activity against drug-resistant panel of *S. aureus* (MIC 8 mg/L) and *Enterococcus spp* (32 mg/L) and exhibits concentration-dependent bacterial killing. AE4G0 synergized with gentamicin, showing better bacterial load reduction than individual treatment groups against *S. aureus* ATCC 29213 and gentamicin-resistant MRSA NRS119. As reported earlier, *S. aureus* can potentially become resistant to all classes of antibiotics currently in therapeutic regime, either by mutation or by acquiring horizontally transferred resistance factors[37]. AE4G0 fails to induce resistance in S. aureus ATCC 29213 whereas levofloxacin under the same conditions, develops stable, high-level resistance. In addition, AE4G0 has a long PAE of ~15.5 h, an essential asset for a new molecule as it reduces the dosages required for therapeutic clearance.

Biofilm formation is a natural phenomenon found in most bacteria; strong adhesion and drug resistance are one of the main features of biofilms, which help bacteria to neutralize the host immune response and escape antibiotic killing[38].

We report AE4G0 has the potential to eradicate the *S. aureus* biofilm significantly, which is an essential aspect for a new drug entity. When analysed by fluorescence microscopy, dead cells were more prominent as compared to untreated after the treatment of *S. aureus* ATCC 29213 with 10x MIC of AE4G0 for 1h, and in the case of SEM, intracellular debris coming out of the lysed cells visible when *S. aureus* ATCC 29213 treated with 10x MIC of AE4G0 for 1h. When tested in the murine skin infection model, AE4G0 reduced bacterial load by ~1.2 $\log_{10}$ CFU/gm compared to untreated *S. aureus* ATCC 29213. When AE4G0 was combined with gentamicin, the combination showed better reduction than the individual treatments and reduced ~0.7 $\log_{10}$ CFU/gm bacterial load compared to untreated gentamicin-resistant *S. aureus* NRS119. When used in combination, AE4G0 reduces the Gentamicin dose for treatment, thus further helping in reduction of gentamicin dosages in treatment of topical infections.

Conclusion

Discovery and development of new antimicrobials is an urgent medical need calling for significant innovation. Dendrimers represent an unconventional strategy since their most common utilization is as carrier or cargo of drugs and or other molecules such as dendriplexes with siRNA, mRNA, etc. In marked contrast, *active per* se antimicrobial properties of dendrimers are poorly documented. Although phosphorus dendrimers are very active against various diseases, very few reported dendrimers demonstrating activity against *S. aureus*, but none were from generation 0[39, 40]. The problem associated with polycationic dendrimers is their toxicity to eukaryotic cells[41]; dendrimers with low molecular mass are known for their lower toxicity than dendrimers with high molecular mass[42]. Thus, in this context, this work reports the first example of direct antimicrobial activity *per se* of a small dendrimer of generation 0 against S. *aureus* ATCC 29213 along with in vivo activity alone and in combination with gentamicin against gentamicin-resistant MRSA NRS119. Considering its excellent antimicrobial properties, AE4G0 has the potential to be translated into a novel therapeutic strategy targeting drug-resistant *S. aureus* topical infections.

Acknowledgements: S.M.: This work was supported by FCT-Fundação para a Ciência e a Tecnologia through the CQM Base Fund - UIDB/00674/2020 and Programmatic Fund- UIDP/00674/2020 and by ARDITI-Agência Regional para o Desenvolvimento da InvestigaçãoTecnologia e Inovação through funds from RegiãoAutónoma da Madeira-Governo Regional) J.P. Majoral, E. Apartsin, R. Laurent thank CNRS for financial support. This study was supported by CSIR Intramural funds to SC. GK thanks DST INSPIRE while AA and DS thank UGC for their fellowship. The following reagents were provided by Network on Antimicrobial Resistance in *Staphylococcus aureus* (NARSA) for distribution by BEI

Resources, NIAID, NIH: NR100, NR119, NR129, NR186, NR191, NR192, NR193, NR194, NR198, VRS1, VRS4, VRS12, NR31884, NR31885, NR31886, NR31887, NR31888, NR31903, NR31909 and NR31912. This manuscript bears CSIR-CDRI communication number ....

Ethics approval: The use of mice for infectious studies (IAEC/2019/2/Renew-1/Dated-22.06.2020) was approved by Institutional Animal Ethics Committee at CSIR-CDRI, Lucknow.

Competing financial interests: The authors declare no competing financial interests.

Transparency declarations: None to declare

Supporting information files:

S1 synthesis of monomers, ^{1}H, ^{13}C NMR spectra, HRMS of compound AE4G0

S2 MIC of dendrimers against gram-positive and gram-negative bacteria.

S3 PMBN assay for AE4G0.

S4 Antibiogram of *S. aureus* ATCC 29213 grown in presence of AE4G0 and Levofloxacin for 35th passage.

References:

1. Kaul, G., et al., *Update on drug-repurposing: is it useful for tackling antimicrobial resistance?* 2019, Future Medicine. p. 829-831.
2. Guo, Y., et al., *Prevalence and therapies of antibiotic-resistance in Staphylococcus aureus.* Frontiers in cellular and infection microbiology, 2020. **10**: p. 107.
3. World Health Organisation. *Antimicrobial resistance*. 2021 [cited 2023 February 04]; Available from: www.who.int/news-room/fact-sheets/detail/antimicrobial-resistance.
4. World Health Organisation. *WHO publishes list of bacteria for which new antibiotics are urgently needed*. 2017 [cited 2023 February 5]; Available from: www.who.int/news/item/27-02-2017-who-publishes-list-of-bacteria-for-which-new-antibiotics-are-urgently-needed.

5. Worley, B.V., D.L. Slomberg, and M.H. Schoenfisch, *Nitric oxide-releasing quaternary ammonium-modified poly (amidoamine) dendrimers as dual action antibacterial agents.* Bioconjugate chemistry, 2014. **25**(5): p. 918-927.
6. Meyers, S.R., et al., *Anionic amphiphilic dendrimers as antibacterial agents.* Journal of the American Chemical Society, 2008. **130**(44): p. 14444-14445.
7. Galanakou, C., D. Dhumal, and L. Peng, *Amphiphilic dendrimers against antibiotic resistance: light at the end of the tunnel?* Biomaterials Science, 2023.
8. Mignani, S., et al., *Multivalent Copper (II)-Conjugated Phosphorus Dendrimers with Noteworthy In Vitro and In Vivo Antitumor Activities: A Concise Overview.* Molecular Pharmaceutics, 2021. **18**(1): p. 65-73.
9. Mignani, S., et al., *In vivo therapeutic applications of phosphorus dendrimers: State of the art.* Drug Discovery Today, 2021. **26**(3): p. 677-689.
10. Chen, L., et al., *Engineered Stable Bioactive Per Se Amphiphilic Phosphorus Dendron Nanomicelles as a Highly Efficient Drug Delivery System To Take Down Breast Cancer In Vivo.* Biomacromolecules, 2022. **23**(7): p. 2827-2837.
11. Mignani, S., et al., *Safe Polycationic Dendrimers as Potent Oral In Vivo Inhibitors of Mycobacterium tuberculosis: A New Therapy to Take Down Tuberculosis.* Biomacromolecules, 2021. **22**(6): p. 2659-2675.
12. Blanzat, M., et al., *Dendritic catanionic assemblies: in vitro anti-HIV activity of phosphorus-containing dendrimers bearing Galß1cer analogues.* ChemBioChem, 2005. **6**(12): p. 2207-2213.
13. Blattes, E., et al., *Mannodendrimers prevent acute lung inflammation by inhibiting neutrophil recruitment.* Proceedings of the National Academy of Sciences, 2013. **110**(22): p. 8795-8800.
14. Fruchon, S., et al., *Anti-inflammatory and immunosuppressive activation of human monocytes by a bioactive dendrimer.* Journal of Leucocyte Biology, 2009. **85**(3): p. 553-562.
15. Hayder, M., et al., *A phosphorus-based dendrimer targets inflammation and osteoclastogenesis in experimental arthritis.* Science translational medicine, 2011. **3**(81): p. 81ra35-81ra35.

16. Posadas, I., et al., *Neutral high-generation phosphorus dendrimers inhibit macrophage-mediated inflammatory response in vitro and in vivo.* Proceedings of the National Academy of Sciences, 2017. **114**(37): p. E7660-E7669.
17. Klajnert, B., et al., *EPR study of the interactions between dendrimers and peptides involved in Alzheimer's and prion diseases.* Macromolecular bioscience, 2007. **7**(8): p. 1065-1074.
18. Apartsin, E., et al., *Dendriplex-Impregnated Hydrogels with Programmed Release Rate.* Frontiers in Chemistry, 2022. **9**: p. 1195.
19. Wrońska, N., et al., *Synergistic effects of anionic/cationic dendrimers and levofloxacin on antibacterial activities.* Molecules, 2019. **24**(16): p. 2894.
20. Wayne, P., *Clinical and Laboratory Standards Institute: Performance standards for antimicrobial susceptibility testing: 20th informational supplement.* CLSI document M100-S21, 2012.
21. Ferrer-Espada, R., et al., *A permeability-increasing drug synergizes with bacterial efflux pump inhibitors and restores susceptibility to antibiotics in multi-drug resistant Pseudomonas aeruginosa strains.* Scientific reports, 2019. **9**(1): p. 3452.
22. Vaara, M., *Polymyxin derivatives that sensitize Gram-negative bacteria to other antibiotics.* Molecules, 2019. **24**(2): p. 249.
23. Twentyman, P.R. and M. Luscombe, *A study of some variables in a tetrazolium dye (MTT) based assay for cell growth and chemosensitivity.* British journal of cancer, 1987. **56**(3): p. 279-285.
24. Thakare, R., et al., *Repurposing disulfiram for treatment of Staphylococcus aureus infections.* International journal of antimicrobial agents, 2019. **53**(6): p. 709-715.
25. Thakare, R., et al., *Repurposing Ivacaftor for treatment of Staphylococcus aureus infections.* International journal of antimicrobial agents, 2017. **50**(3): p. 389-392.
26. Odds, F.C., *Synergy, antagonism, and what the chequerboard puts between them.* Journal of Antimicrobial Chemotherapy, 2003. **52**(1): p. 1-1.

27. Kwasny, S.M. and T.J. Opperman, *Static biofilm cultures of Gram-positive pathogens grown in a microtiter format used for anti-biofilm drug discovery.* Current protocols in pharmacology, 2010. **50**(1): p. 13A. 8.1-13A. 8.23.

28. Suller, M. and D. Lloyd, *The antibacterial activity of vancomycin towards Staphylococcus aureus under aerobic and anaerobic conditions.* Journal of applied microbiology, 2002. **92**(5): p. 866-872.

29. Tambe, S., L. Sampath, and S. Modak, *In vitro evaluation of the risk of developing bacterial resistance to antiseptics and antibiotics used in medical devices.* Journal of Antimicrobial Chemotherapy, 2001. **47**(5): p. 589-598.

30. Kugelberg, E., et al., *Establishment of a superficial skin infection model in mice by using Staphylococcus aureus and Streptococcus pyogenes.* Antimicrobial agents and chemotherapy, 2005. **49**(8): p. 3435-3441.

31. Apartsin, E.K., et al., *Hydrogels of Polycationic Acetohydrazone-Modified Phosphorus Dendrimers for Biomedical Applications: Gelation Studies and Nucleic Acid Loading.* Pharmaceutics, 2018. **10**(3): p. 120.

32. El Ghzaoui, A., et al., *Self-assembly of water-soluble dendrimers into thermoreversible hydrogels and macroscopic fibers.* Langmuir, 2004. **20**(21): p. 9348-9353.

33. Majoral, J., et al., *Heterocycles contenant du phosphore? XXIX.* Tetrahedron, 1976. **32**(21): p. 2633-2644.

34. Flamm, R.K., et al., *Evaluation of the bactericidal activity of fosfomycin in combination with selected antimicrobial comparison agents tested against Gram-negative bacterial strains by using time-kill curves.* Antimicrobial agents and chemotherapy, 2019. **63**(5): p. e02549-18.

35. Belley, A., et al., *Assessment by time-kill methodology of the synergistic effects of oritavancin in combination with other antimicrobial agents against Staphylococcus aureus.* Antimicrobial agents and chemotherapy, 2008. **52**(10): p. 3820-3822.

620 36. Petersen, P.J., et al., *In vitro antibacterial activities of tigecycline in combination with other*
621 *antimicrobial agents determined by chequerboard and time-kill kinetic analysis.* Journal of
622 Antimicrobial Chemotherapy, 2006. **57**(3): p. 573-576.
623 37. Vestergaard, M., D. Frees, and H. Ingmer, *Antibiotic resistance and the MRSA problem.* Microbiology
624 spectrum, 2019. **7**(2): p. 7.2. 18.
625 38. Kanwar, I., A. K Sah, and P. K Suresh, *Biofilm-mediated antibiotic-resistant oral bacterial infections:*
626 *mechanism and combat strategies.* Current pharmaceutical design, 2017. **23**(14): p. 2084-2095.
627 39. Altaher, Y. and M. Kandeel, *Structure-Activity Relationship of Anionic and Cationic Polyamidoamine*
628 *(PAMAM) Dendrimers against Staphylococcus aureus.* Journal of Nanomaterials, 2022. **2022**.
629 40. Lopez, A.I., et al., *Antibacterial activity and cytotoxicity of PEGylated poly (amidoamine) dendrimers.*
630 Molecular BioSystems, 2009. **5**(10): p. 1148-1156.
631 41. Padié, C., et al., *Polycationic phosphorus dendrimers: synthesis, characterization, study of*
632 *cytotoxicity, complexation of DNA, and transfection experiments.* New Journal of Chemistry, 2009.
633 **33**(2): p. 318-326.
634 42. Klajnert, B., et al., *Biological properties of low molecular mass peptide dendrimers.* International
635 journal of pharmaceutics, 2006. **309**(1-2): p. 208-217.

636

637 **Table 1**: MIC (mg/L) of AE4G0 against ESKAPE Pathogens

Strains				**Antibiotics resistant to**	**Molecular details of strains**	**MIC of AE4G0 (mg/L)**
Gram-positive bacteria	MSSA	*S. aureus*	ATCC 29213	None	Type strain	8
	MRSA		NRS100	Methicillin, Tetracycline	Contains subtype I mec cassette & large variety of virulence factors	8
			NRS119	Methicillin, Gentamicin, Linezolid, Trimethoprim / sulfamethaxazole	Contains subtype IV mec cassette & G2576T mutation in domain V in one or more 23S rRNA genes	8

			NRS129	Chloramphinecol	*mecA* negative	8
			NRS186	Methicillin, Levofloxacin, Meropenem	USA 300 type CA-MRSA, PVL virulence factor positive & contains *mec* type IV cassette	8
			NRS191	Methicillin, Levofloxacin, Meropenem	USA 600 type CA-MRSA, PVL virulence factor negative & contains *mec* type II cassette	8
			NRS192	Methicillin, Levofloxacin, Meropenem, Erythromcyin	CA-MRSA, PVL virulence factor negative & contains *mec* type II cassette	8
			NRS193	Methicillin, Levofloxacin, Meropenem	CA-MRSA, PVL factor negative & contains *mec* type II cassette	8
			NRS194	Methicillin, Meropenem	CA-MRSA, PVL virulence factor positive & contains mec type V cassette	8
			NRS198	Methicillin, Levofloxacin, Meropenem	USA 100 type CA-MRSA, PVL virulence factor negative & contains *mec* type II cassette	16
	VRSA		VRS 1	Methicillin, Levofloxacin, Meropenem,Vancomycin, Gentamycin, Teicoplanin & Spectinomycin	USA 100, contains *mec* subtype II cassette &*vanA,* Negative for *vanB*, *vanC1*, *vanC2*, *vanD*, *vanE*, PVL & ACME	8
			VRS 4	Methicillin, Levofloxacin, Meropenem, Vancomycin, Gentamycin, Teicoplanin & Spectinomycin	USA 100, contains mec subtype II cassette & *vanA,* Negative for *vanB*, *vanC1*, *vanC2*, *vanD*, *vanE*, PVL & ACME	8
			VRS 12	Methicillin, Levofloxacin, Meropenem, Vancomycin, Gentamycin, Teicoplanin & Spectinomycin	Data not available	8
	Enterococcus		NR31884	Methicillin, Gentamicin	Hemolytic, cytolytic isolate	32
			NR31885	Methicillin, Gentamicin	Cytolytic isolate	32
			NR31886	Methicillin, Gentamicin	Hemolytic isolate	32
			NR31887	Methicillin, Gentamicin, Minocycline	None	32
			NR31888	Methicillin, Gentamicin	Cytolytic isolate	32
Gram-negative bacteria	*Escherichia coli* ATCC 25922			None	Type strain	>64
	Klebsiella pneumoniae BAA-1705			Carbapenem-resistant (Imipenem and Ertapenem)	Type strain	>64
	Acinetobacter baumannii BAA-1605			Ceftazidime, Gentamicin, Ticarcillin, Piperacillin, Aztreonam, Cefepime, Ciprofloxacin, Imipenem and Meropenem	Type strain	>64
	Pseudomonas aeruginosa ATCC 25923			None	Type strain	>64
	Enterobacter cloacae complex Strain NR 50394			Azithromycin, Clarithromycin, Phosphomycin and Minocycline	Isolated as nosocomial pathogens	>64
	Enterobacter cloacae			Azithromycin, Ciprofloxacin,	Isolated as nosocomial	>64

	complex Strain NR 50399	Clarithromycin, Carbenicillin, Levofloxacin, Moxifloxacin, Phosphomycin & Trimethoprim	pathogens	638 639 640 641
	Enterobacter cloacae complex Strain NR 50401	Ceftriaxone, Ciprofloxacin, Levofloxacin, Phosphomycin, Moxifloxacin, Trimethoprim, Cefoprazone & Aztreonam	Isolated as nosocomial pathogens	642 643 >64 644 645 646

647 MSSA: Methicillin Susceptible *Staphylococcus aureus*, MRSA:Methicillin Resistance *Staphylococcus aureus*, VRSA:Vancomycin Resistance
648 *Staphylococcus aureus*, PVL: Panton-Valentine leucocidin virulence factor, ACME: arginine catabolic mobile element, CA: Community-acquired
649

650 Table 2: Cytotoxicity of Synthesized dendrimers against Vero cells (ATCC CCL-81).

651

652

Compound	MIC (mg/L)	CC_{50} (mg/L)	Selectivity Index (CC_{50}/MIC)	653 654
AE4G0	8	>250	>31.25	655
TG0L	4	>200	>50	656
Net3G0L	4	>200	>50	657
C5MeG0L	4	>200	>50	658
PG0L	8	>200	>25	659
C6MeG0L	4	>200	>50	660
C5MeG0	16	>200	>12.5	661
C6MeG0	16	>200	>12.5	662
C5HG0	32	100	3.125	663
NEt3G0	8	>200	>25	664 665

666 Table 3: Drug interaction of AE4G0 with FDA-approved drugs against *Staphylococcus aureus* ATCC 29213

Drug	MIC of Drug alone (mg/L)	MIC of drug in presence of AE4G0 (mg/L)	MIC of AE4G0 alone (mg/L)	MIC of AE4G0 in presence of drug (mg/L)	FIC Index	Indication
Ceftazidime	8	8	8	8	2	No interaction
Daptomycin	1	2	8	8	3	No interaction
Gentamicin	0.25	0.125	8	2	0.75	No interaction
Linezolid	2	2	8	8	2	No interaction
Levofloxacin	0.25	0.25	8	8	2	No interaction
Meropenem	0.125	0.125	8	8	2	No interaction
Minocycline	0.125	0.125	8	8	2	No interaction

Rifampicin	0.0078	0.0078	8	8	2	No interaction
Vancomycin	1	1	8	8	2	No interaction

667

668 Table 4: Post Antibiotic Effect studies for AE4G0

Treatments	Time for 1 log_{10}(h)	PAE (h)
Untreated *S. aureus* ATCC 29213	~2	0
AE4G0 1x	~2	~0
AE4G0 10x	~17.5	~15.5
Vancomycin 1x	~3	~1
Vancomycin 10x	~4	~2

669

670 Fig 2: (a) Time Kill kinetics of AE4G0 against *S. aureus* ATCC 29213 along with comparators (b) Time Kill kinetics of
671 AE4G0 + Gentamicin against *S. aureus* ATCC 29213 along with comparators (c) Time Kill kinetics of AE4G0 and
672 Gentamicin against gentamicin resistant *S. aureus* NRS119

673

674 (a)

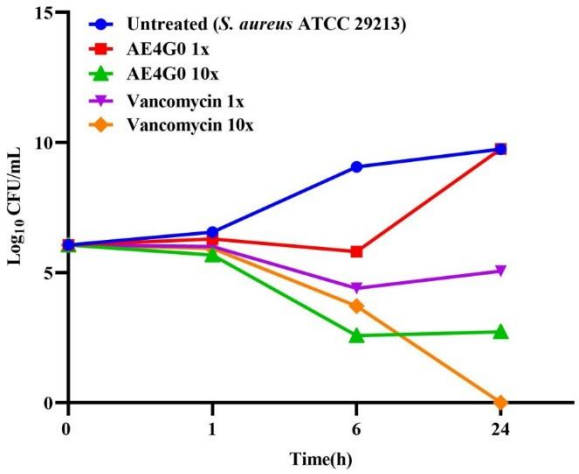

675

676

677

678

679

680

681

682 (b)

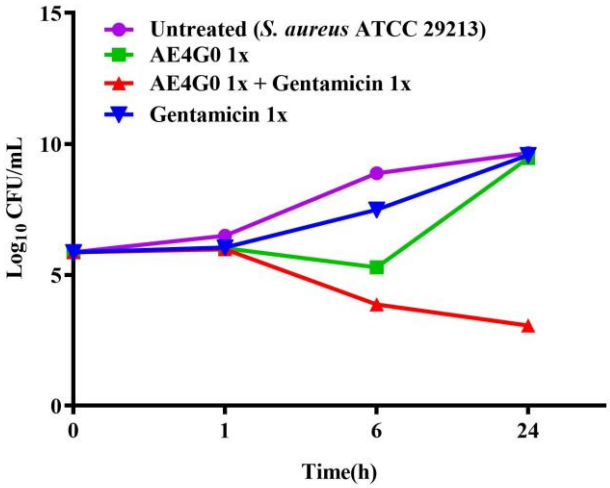

683

(c)

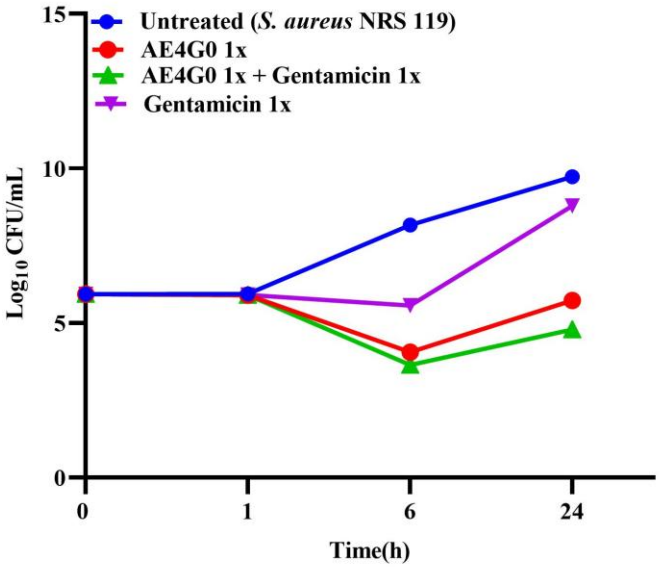

Fig 3: Activity of AE4G0, vancomycin and levofloxacin against pre-formed *S. aureus* ATCC 29213 biofilm.

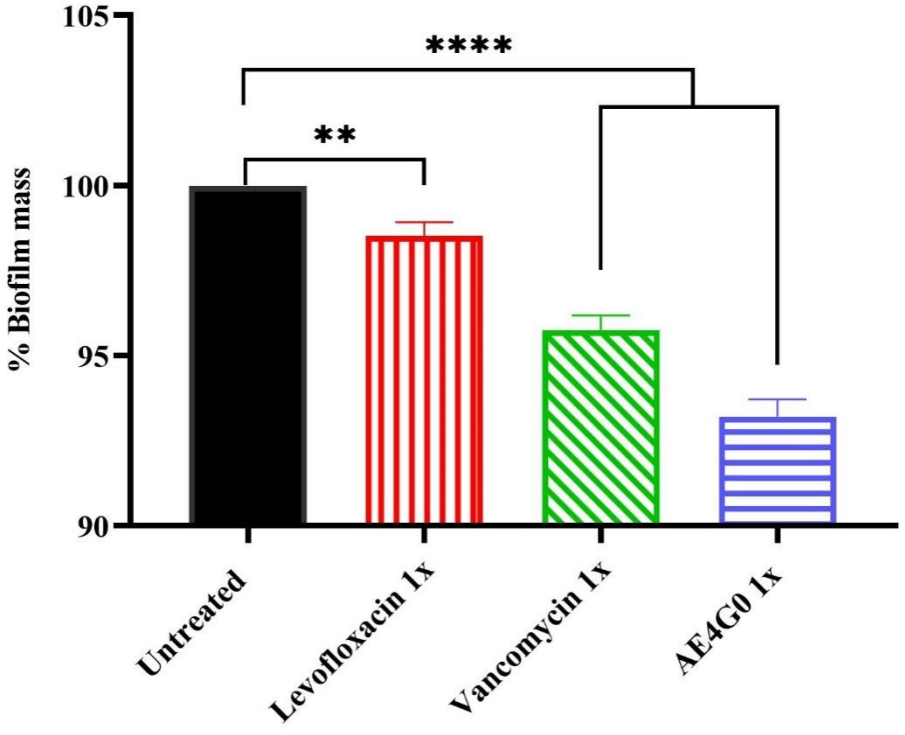

Fig 4: Induction of resistance against AE4G0 and levofloxacin in *S. aureus* ATCC 29213 at sub-inhibitory concentrations.

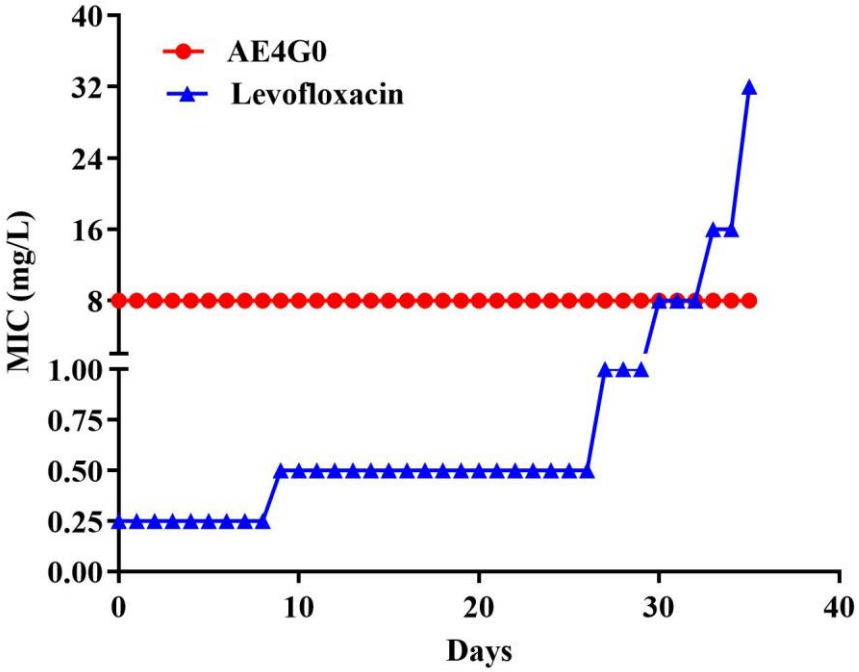

Fig 5: Confocal and SEM analysis of *S. aureus* ATCC 29213 treated with AE4G0 at 10x MIC for 1h. The cells were exposed to AE4G0 and treated with Bacterial viability stain and prepared for SEM. Viable bacterial cells were stained green by SYTO9 whereas dead cells were stained red by PI.

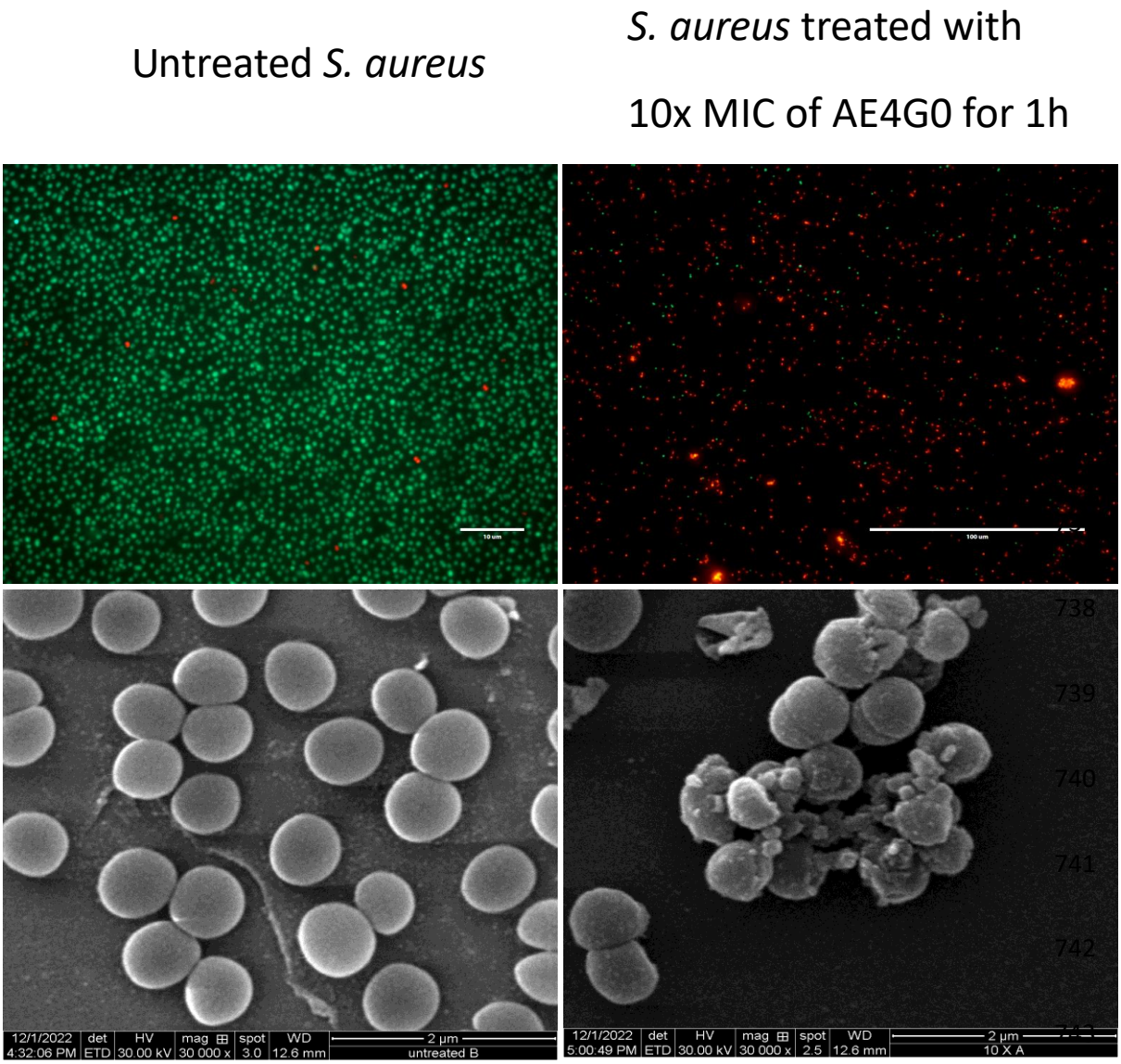

Fig 6: (a) *In vivo* efficacy of AE4G0 against *S. aureus* ATCC 29213 in a murine skin infection model. (b) *In vivo* efficacy of AE4G0 against gentamicin-resistant *S. aureus* ATCC NRS119 in a murine skin infection model.

(a)

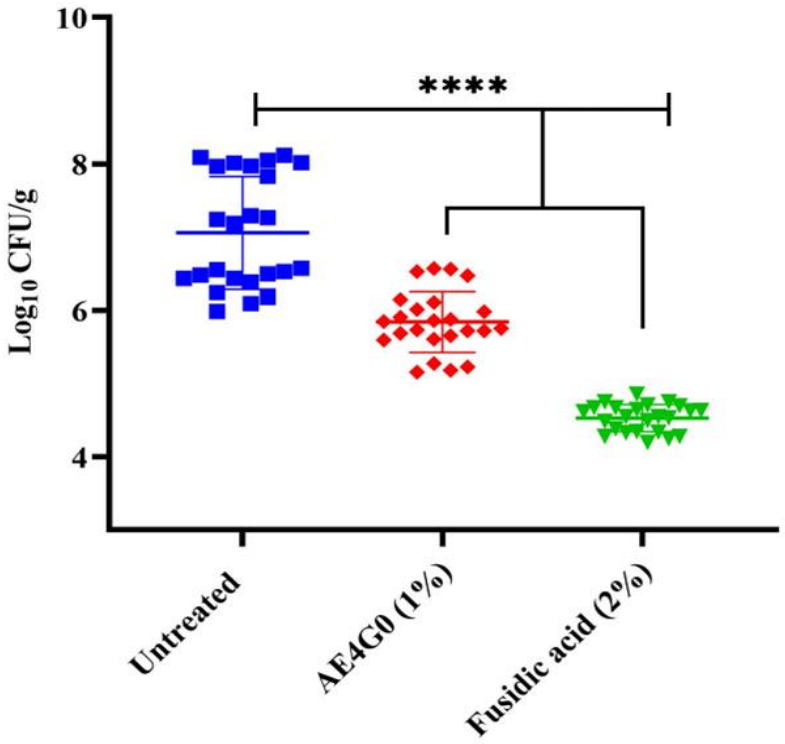

(b)